# Engraftment of Neonatal Lung Fibroblasts into the Normal and Elastase-Injured Lung

**Ping-Ping Kuang, Edgar Lucey, David C. Rishikof, Donald E. Humphries, Daniel Bronsnick, and Ronald H. Goldstein**

Pulmonary Center, Boston University School of Medicine, and the VA Boston Healthcare System, Boston, Massachusetts

**Interstitial fibroblasts are an integral component of the alveolar wall. These cells produce matrix proteins that maintain the extracellular scaffold of alveolar structures. Emphysema is characterized by airspace enlargement resulting from the loss of alveolar cellularity and matrix. In this study, we explored the endotracheal delivery of fibroblasts to the lung parenchyma as a means of repairing damaged alveolar structures directly or indirectly for the delivery of transgenes. Fibroblasts were isolated from the lungs of neonatal transgenic mice expressing GFP during the period of rapid alveolarization. These $GFP^+$ cells maintained their myofibroblast phenotype in culture and expressed elastin and α-smooth muscle actin mRNA. We administered $GFP^+$ fibroblasts to saline- and elastase-treated mice by endotracheal instillation. We detected more $GFP^+$ fibroblasts in the alveolar walls and in the interstitial areas of elastase-injured lungs than in normal lungs as assessed by immunohistochemistry and fluorescent imaging. The presence of $GFP^+$ fibroblasts in the interstitium demonstrated transepithelial migration of these cells. Expression of $GFP^+$ fibroblasts in recipient lungs was maintained for at least 20 d after endotracheal administration. These cells synthesize matrix components including elastin *in vitro* and could contribute to restoring the structural integrity of the alveolar wall.**

**Keywords:** elastase; elastin; emphysema; fibroblasts

Emphysema is defined by the presence of airspace enlargement (1, 2). The occurrence of emphysema in patients with $\alpha_1$-antitrypsin inhibitor deficiency indicates that destruction of matrix substances especially elastin and collagen is an important feature of this process. Failure to repair damaged elastin may also contribute to airspace enlargement. Mice deficient in lysyl oxidase–like protein 1 (LOXL1) develop airspace enlargement in adult life (3). This enzyme promotes the formation of crosslinks between elastin fibrils in the developing fiber and is a component of the extracellular scaffold providing structural support to alveolar walls. The elastin and collagen network is subject to remodeling, presumably by synthesis and incorporation of newly formed fibrils into damaged fibers. The failure to maintain elastin renewal in the alveolar wall results in loss of structural integrity. Similarly, mice deficient in fibulin-5 develop airspace enlargement. This extracellular protein binds elastin and LOXL1 and may be important in the organization of the extracellular scaffold (4).

Emphysema in mice can be induced by endotracheal administration of pancreatic or neutrophil elastase (2). Levels of lung elastin initially decrease after endotracheal administration of elastase, but return to normal levels over the course of several weeks (5). Using this model of emphysema, we previously demonstrated that elastin mRNA is upregulated in the large vascular tissues and minimally expressed in the walls of respiratory air spaces at the free margins of alveolar septa (6). However, the deposition of elastin did not restore normal alveolar architecture. In addition, the formation of new alveolar units did not occur after injury as assessed by *in situ* hybridization (6). The loss of interstitial fibroblasts and supporting structures may preclude the restitution of normal alveolar architecture.

We have previously isolated myofibroblasts from the neonatal lung at the time of rapid alveoli formation (Days 7–14) (9–12). These cells synthesize elastin and collagen and respond to inflammatory mediators, especially interleukin (IL)-1β (9, 10). Small numbers of fibroblasts have been recovered by bronchoalveolar lavage from individuals with interstitial lung diseases, suggesting that fibroblasts can migrate into and out of alveolar spaces (7, 8). We hypothesized that endotracheally administered fibroblasts could engraft in the lung parenchyma to repair damaged alveolar structures or to deliver transgenes. To determine whether fibroblasts would localize to injured alveolar walls, we endotracheally administered lung fibroblasts isolated from neonatal transgenic mice expressing GFP into adult normal and elastase-treated mice. We found that these $GFP^+$ fibroblasts engrafted in the alveolar interstitium.

## MATERIALS AND METHODS

### Materials and Cell Culture

Neonatal lung fibroblasts also referred to as lung interstitial cells (LIC) were isolated from the lungs of 10-d-old C57BL/6J and green florescent protein (GFP)-expressing transgenic mice (C57BL/6(ACTbEGFP) 1Osb/J; Jackson Laboratory, Bar Harbor, ME) by digestion with 0.25% typsin IX and collagenase type II (Sigma-Aldrich, St. Louis, MO) as previously described (9, 10). The enhanced GFP cDNA is under the control of a chicken β-actin promoter and cytomegalovirus enhancer, and causes all tissues with the exception of erythrocytes to appear green under excitation light. After isolation, LIC were grown in minimal essential medium (MEM; Invitrogen, Carlsbad, CA) with 10% fetal bovine serum (FBS) and cultured in T-75 $cm^2$ flasks (Falcon Plastics, Los Angeles, CA). Cultures were maintained in a humidified 5% $CO_2$, 95% air incubator at 37°C for 3–5 d until confluence. Cells were trypsinized, washed twice with PBS, and resuspended in PBS at $5 \times 10^6$ cells per ml. Each animal was administered fibroblasts at $5 \times 10^5$/0.1 ml by endotracheal instillation. The percentage of lipid containing fibroblasts in the cultures was assessed using phase microscopy and Oil Red O staining (Fisher Scientific, Springfield, NJ).

### Treatment

Wild-type, C57BL/6J adult mice (Jackson Laboratory) were anesthetized with methoxyflurane (Metofane; Pitman Moore, Mundelein, IL) and given an endotracheal instillation of 30 μg porcine pancreatic elastase (Elastin Products, St. Louis, MO) in 0.1 ml of sterile saline solution (0.9% NaCl) or 0.1 ml of saline alone. The animal protocols were reviewed and approved by the animal studies committee at the Boston VA Medical Center.

(*Received in original form October 8, 2004 and in final form May 15, 2005*)

This work was supported by the Department of Veterans Affairs REAP research program and the National Heart, Lung, and Blood Institute Grants HL66547 and HL46902.

Correspondence and requests for reprints should be addressed to Ronald H. Goldstein, M.D., The Pulmonary Center, Boston University School of Medicine, 715 Albany Street, R-304 Boston, MA 02118. E-mail: rgoldstein@lung.bumc.bu.edu

**Am J Respir Cell Mol Biol Vol 33. pp 371–377, 2005**
**Originally Published in Press as DOI: 10.1165/rcmb.2004-0319OC on July 21, 2005**
**Internet address: www.atsjournals.org**

### Preparation of Tissue

Groups of mice were killed for study at either 5 or 20 d after treatment. Animals were anesthetized with pentobarbital sodium and exsanguinated by cutting the abdominal aorta. The lungs were inflated with freshly prepared paraformaldehyde and excised. Slabs of tissue were cut from the lung and dehydrated and embedded in Paraplast Plus (Oxford Laboratories, St. Louis, MO) embedding medium. Four-micron serial paraffin sections were cut, individually handled and numbered, and transferred to Superfrost Plus slides (Fisher Scientific).

### Immunohistochemistry

Lung was inflation-fixed with 4% paraformaldehyde, dehydrated in ethanol, and embedded in paraffin. Primary antibodies used for immunohistochemistry include F4/80, rat anti-mouse (Serotec Inc, Raleigh, NC), α-smooth muscle actin (α-SMA), mouse monoclonal and isotype control IgG2 (Sigma-Aldrich), GFP, rabbit polyclonal (Molecular Probes, Eugene, OR), and CD45, rat anti-mouse (BD Pharmingen, San Jose, CA). Deparaffinized tissue sections were blocked with nonimmune rabbit sera, incubated with the antibodies at various dilutions, rinsed, and stained for peroxidase activity with the Vectabond ABC kit or Histomouse max sample Kit (α-SMA) (Zymed Lab, San Francisco, CA). Unstained sections or sections stained with dilute hematoxylin were photographed in a Leitz Orthoplan microscope (Solms, Germany). Isotype control antibodies were employed as negative controls. Photographs were generated with the Improvision Open-Lab Users Software program (Quincy, MA).

### Fluorescent Imaging

Unstained paraffin sections were examined for green fluorescence using a Nikon Eclipse E600 microscope (Melville, NY) with epifluorescence attachment and a Triple (D-F-T) filter block. Digital photomicrographs were taken with a RT Slider camera (Diagnostic Instruments, Sterling Heights, MI).

### Morphometry

Quantitative histologic measurements were made with an image analysis system, consisting of a Nikon E600 microscope, a Spot RT Slider digital camera and a computer with Image-Pro Plus image analysis software. Six fields from 4-μm-thick tissue sections of each mouse lung were photographed. From each photographed field, five areas were picked by a random process for measurement of the number of intersections of virtual lines of known length, with alveolar septa. The areas were free of airways and muscular blood vessels. An increase in the average distance between intercepts (mean linear intercept [MLI]) indicates enlarged airspaces.

### RNA Isolation and Northern Blot Analysis

Total RNA was prepared using the RNeasy mini kit (Qiagen, Valencia, CA) according to the manufacturer's protocol. Equal amount of RNA (10 μg/lane) was electrophoresis in 1% agarose gel with formaldehyde and transferred to a Hybond N+ membrane (Amersham, Piscataway, NJ). The RNA membrane was ultravioletly cross-linked and hybridized with $^{32}$P-labeled cDNA probes for elastin, α-SMA or an oligonucleotides that binds the 18S ribosome subunit in Rapid Hybridization Buffer (Amersham), followed by washing twice in 2× SSC, 0.1% SDS at room temperature (RT) for 15 min and once in 0.1× SSC, 0.1% SDS at 65°C for cDNA probes, and at 37°C for oligonucleotide probes for 20 min. The 18S specific oligonucleotides were synthesized by IDT, Inc. (Coralville, IA).

### Statistics

A Student's *t* test was used for means of unequal size. Probability values $< 0.05$ were considered significant.

## RESULTS

We employed lung fibroblasts isolated from 10-d-old pups of GFP$^+$ transgenic mice for our studies. We first examined the expression of GFP in the lungs of 10-d-old transgenic mice by fluorescence imaging and immunohistochemistry (Figure 1).

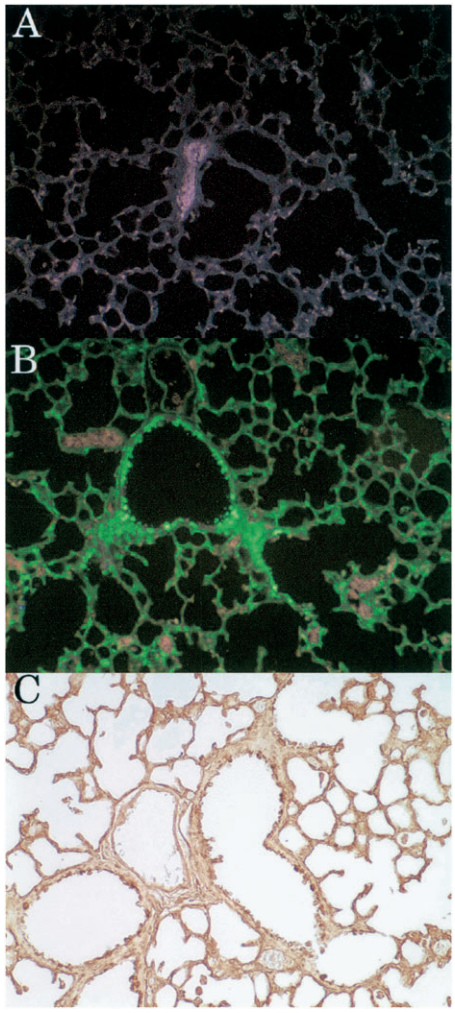


***Figure 1.*** Detection of GFP in 10-d-old mouse pups. (*A*) Unstained lung tissue of a wild-type pup. *B* demonstrates the green fluorescence of the unstained lung of a GFP-transgenic pup that is heterozygous for the GFP gene under the same illumination. It can be seen that most cells of the transgenic lung display the green fluorescence of the GFP. The most notable exceptions are the red blood cells, seen in *B* as *pink-colored cells* within blood vessels. The cells with the greatest fluorescence are in the parenchyma, at the location of type II cells, and in the airway epithelium. *C* demonstrates immunostaining for GFP in a GFP-transgenic lung and detects the same distribution pattern for GFP, as with fluorescence illumination of unstained sections. All panels are the same magnification; short (vertical) dimensions of panels are 436 μm.

GFP was strongly expressed in alveolar cells at this early postnatal time point. We also examined GFP expression in untreated and elastase-treated adult transgenic mice (Figure 2). In the untreated adult lung, GFP expression was observed in all cell types but was more prominent in Type II epithelial cells. Elastase administration induced a characteristic airspace enlargement, but did not change the pattern of GFP expression. To determine whether fibroblasts isolated from neonatal transgenic mice retain GFP expression in culture and after trypsinization, we assessed the fluorescence of these cells and found readily detectable levels of GFP (data not shown). Northern blot analyses revealed abundant expression of elastin and α-SMA mRNA in cultured GFP$^+$ neonatal lung fibroblasts (Figure 3). Treatment with IL-1β decreased the steady-state levels of these mRNA species (Figure 3).

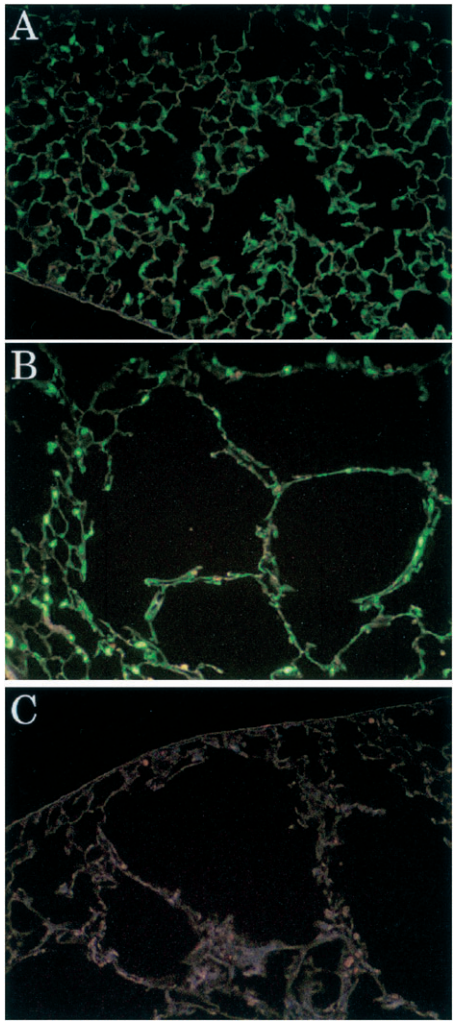


*Figure 2.* Detection of GFP, by fluorescence, in the lungs of adult mice. *A* shows a lung section from a saline-treated transgenic mouse. *B* and *C* show lung sections after PPE-induced injury, of a transgenic and wild-type mouse, respectively. Note the loss of tissue and disruption of normal lung architecture of PPE-treated lungs. There does not appear to be a change in the concentration of highly fluorescent tissue in the injured (emphysematous) areas. All panels are the same magnification; short (vertical) dimensions of panels are 436 μm.

We administered $GFP^+$ neonatal lung fibroblasts by endotracheal instillation to adult wild-type mice at 8 d after endotracheal saline or elastase treatment. At 20 d after the administration of the cell suspension obtained from trypinization of cultured $GFP^+$ fibroblasts, the mice were killed and the lungs were examined for GFP expression using immunohistochemistry (Figure 4). In the saline-treated mice, we detected an occasional $GFP^+$ cell in alveolar structures and in interstitial tissues adjacent to large airways and vascular structures. Review of multiple consecutive sections revealed an average of $0.9 \pm 0.48$ $GFP^+$ cells per section (mean ± SD, $n = 15$ sections). In rare sections, foci of multiple $GFP^+$ cells were present. Similar results were obtained using $GFP^+$ cells immediately after isolation and not cultured from the neonatal lung (data not shown). No $GFP^+$ cells were found in sections from mice that were not administered the cell suspension.

In adult wild-type mice treated with elastase, $GFP^+$ cells were readily detected in the walls of enlarged airspaces (Figure 5).

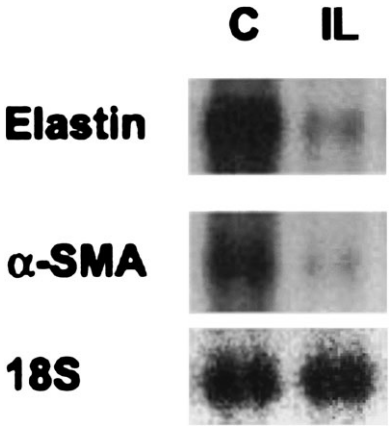


*Figure 3.* Expression of elastin and α-SMA mRNA by neonatal $GFP^+$ cells. Northern analysis of mRNA isolated from cultured $GFP^+$ cells in the presence or absence of IL-1β (IL) at 250 pg/ml. Northern analysis was performed using $^{32}P$-labeled rat elastin cDNA, α-SMA, and an oligonucleotide that binds to the 18S ribosome subunit as probes.

Review of multiple consecutive sections for $GFP^+$ cells from three mice revealed $16.0 \pm 9.7$ $GFP^+$ cells per section (mean ± SD, $n = 30$ sections). The majority of $GFP^+$ cells (79%) were located in abnormal parenchymal areas characterized by disruption of alveolar architecture. To determine whether engraftment of $GFP^+$ cells altered lung morphometry, we measured MLI in lung sections from saline-treated and elastase-treated wild-type mice administered the $GFP^+$ fibroblast suspension (13). The presence of $GFP^+$ did not affect the MLI values in elastase-treated mice ($43.5 \pm 2.0$ in saline-treated, $79.3 \pm 12.0$ in elastase-treated, and $66.9 \pm 21.1$ in elastase-treated with engraftment of $GFP^+$ cells [mean ± SD, $n = 3$]).

To further characterize the phenotype of engrafted $GFP^+$ cells, we examined the lung sections for expression of α-SMA, a protein that is typically expressed by activated fibroblasts (myofibroblasts) and smooth muscle cells (14). We found that in the normal lung, α-SMA was expressed in vascular and airway structures that contain smooth muscle cells (Figure 6). No signal was detected in the parenchyma. After elastase injury, we detected an increase in α-SMA expression in the parenchyma as well as the pleural surface (Figure 6). Inspection of serial lung sections indicated that certain $GFP^+$ cells appear to co-express α-SMA (Figure 7). To verify co-expression of GFP and α-SMA, $GFP^+$ cells were first identified and localized by dark field fluorescence imaging and then α-smooth actin expression was assessed by immunohistochemistry. We found a subpopulation of $GFP^+$ cells that appear to co-express α-SMA (Figure 8).

To determine whether $GFP^+$ cells were derived from a macrophage lineage, we assessed whether $GFP^+$ cells co-express F4/80, a protein specific for mouse macrophages (14). We found that small percentage of $GFP^+$ cells ($< 5\%$) expressed F4/80. These cells were rounded in appearance and resided within the alveolar space. The $GFP^+$ cells that incorporated into alveolar walls were negative for F4/80 (Figure 8) and CD45 (data not shown). To determine whether $F4/80^+$ cells were derived from resident macrophages that ingested GFP material, we administered $GFP^+$ cells that were isolated and rendered nonviable by freeze thawing. We did not detect any $GFP^+$ cells in recipient lungs, indicating that these $GFP^+$ macrophages were derived from the donor lungs.

## DISCUSSION

We postulated that administration of neonatal lung fibroblasts to adult lung could provide a novel approach for repair or delivery of transgenes to injured alveolar structures. Our results demonstrate that neonatal fibroblasts administered endotracheally migrated across epithelial basement membrane and engrafted in

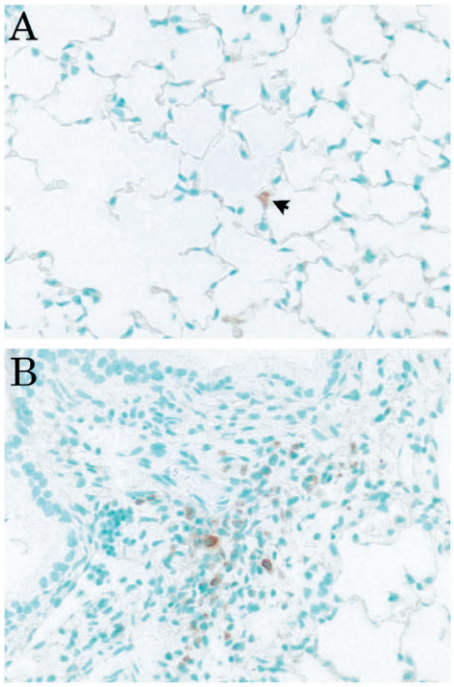


*Figure 4.* Detection of GFP$^+$ cells in the lungs of wild-type host mice 20 d after an intratracheal instillation of cultured GFP$^+$ cells. *A* and *B* show GFP, by immunostaining, in the lung parenchyma. In *A*, an apparent GFP$^+$ cell (*arrow*) is seen within the parenchyma. *B* shows GFP$^+$ cells located in a different section. All panels are the same magnification; short (vertical) dimensions of panels are 218 μm.

the interstitium. Engraftment of fibroblasts in alveolar structures occurred preferentially in areas injured by elastase administration and did not provoke an inflammatory reaction. In some areas, the GFP$^+$ cells appeared within the alveolar wall or alveolar septa. These cells do not co-express F4/80, a macrophage specific protein, or CD45. A subpopulation of engrafted cells expressed α-SMA, a protein expressed by myofibroblasts (15). It is possible that these engrafted cells contribute to matrix accumulation and the structural integrity of the alveolar wall after elastase injury. However, the limited number of engrafted cells did not affect the MLI values in the elastase-injured lung.

Previous studies have demonstrated that small numbers of bone marrow–derived cells injected intravenously into mice can migrate across endothelial and epithelial basement membranes into alveolar structures and display an epithelial type I cell phenotype (16). After bleomycin injury in mice, bone marrow–derived fibroblast-like cells also accumulate in the interstitum (17). These bone marrow stromal cells produce collagen, but do not express α-SMA. Engraftment of immortalized murine fibroblasts into the normal lung was observed after intravenously or endotracheal administration (18). The GFP$^+$ neonatal fibroblasts used in our study were cultivated in conventional culture conditions and did not have the characteristic culture requirements of stem cells. However, a small percentage of GFP$^+$cells were also positive for F4/80, a macrophage specific protein, indicating that the primary fibroblast cultures likely contained limited numbers of other cell types. Engraftment of GFP$^+$ bone marrow cells into the lung and other tissues is associated with low levels of cellular fusion, generating different phenotypes, including epithelial cells (19, 20). Because we employed fibroblast-like cells derived from the neonatal lung, the observed GFP$^+$

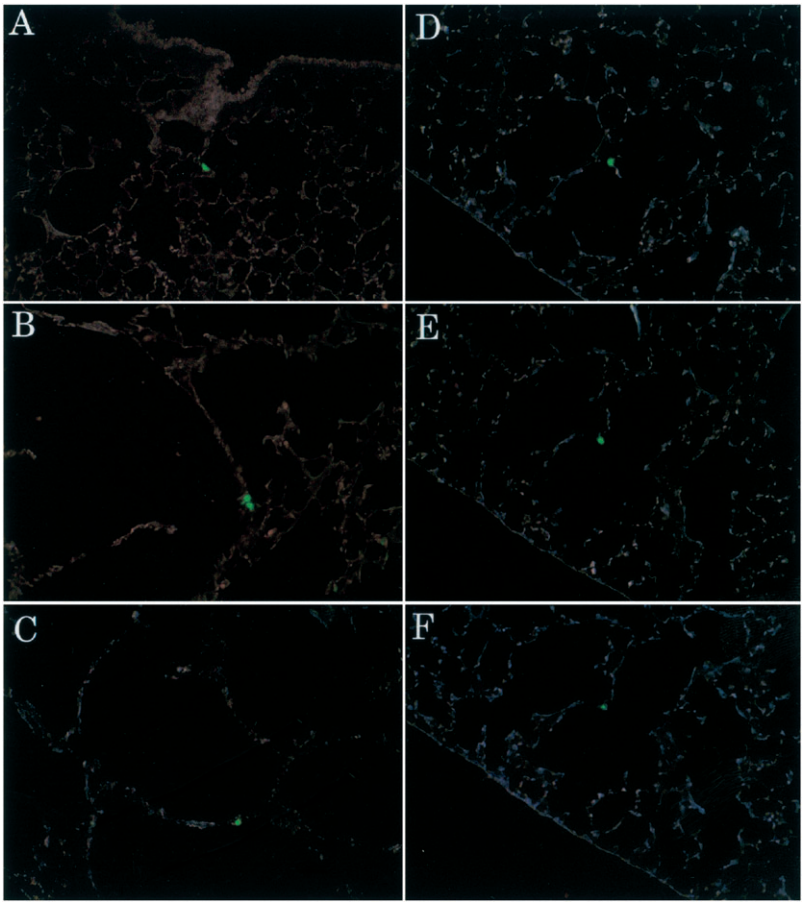


*Figure 5.* Detection of GFP$^+$ cells in the lungs of wild-type PPE-treated host mice 20 d after an intratracheal instillation of cultured GFP$^+$ cells. PPE treatment occurred 10 d before the cell instillation. *A* shows a single GFP$^+$ cell in the lung parenchyma. *B* shows two GFP$^+$ cells in emphysematous tissue. *C* shows a GFP$^+$cell within emphysematous tissue that may contribute to the integrity of the parenchymal structure. *D*, *E*, and *F* show consecutive serial sections of a single cell incorporated into a septal wall. The panels are the same magnification; short (vertical) dimensions of panels are 436 μm.

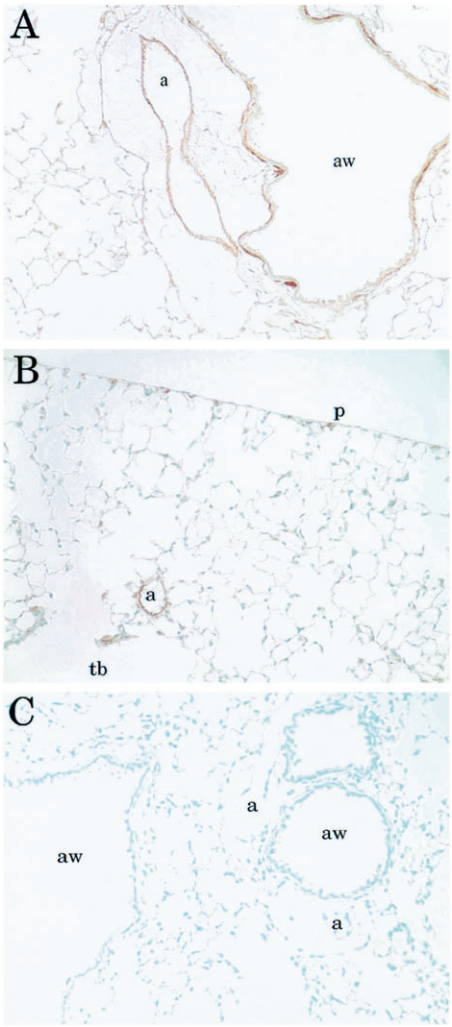


***Figure 6.*** *A* and *B* show α-SMA staining in the smooth muscle of major airway wall (aw), terminal bronchus (tb) and arterial wall (a). α-SMA is also seen in the pleura (p). *C* is an isotype control. All panels are the same magnification; short (vertical) dimensions of panels are 436 μm.

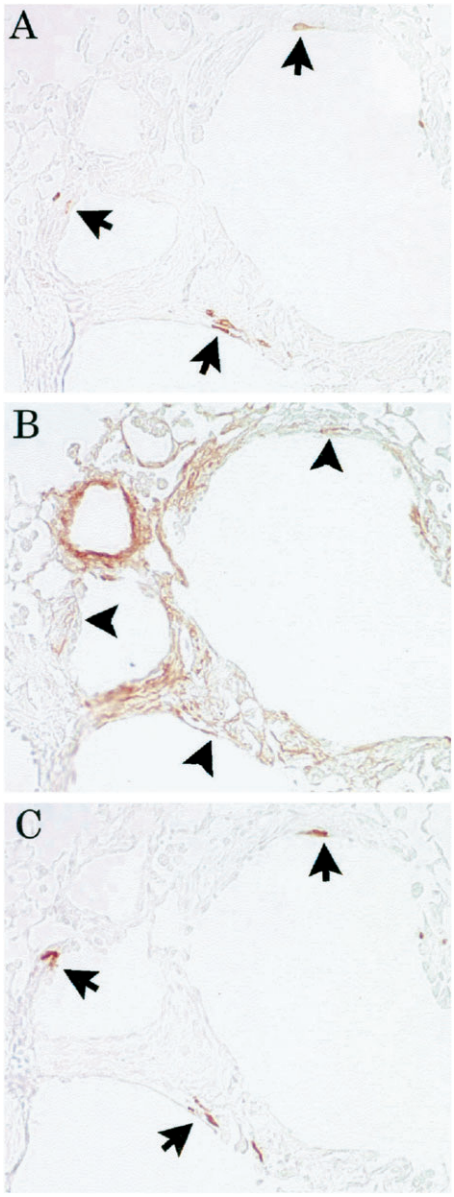


***Figure 7.*** *A, B,* and *C* are from serial 4-μm sections; all showing the same field; *A* and *C* are immunostained for GFP, whereas *B* is immunostained for α-SMA. This wild-type mouse had received $GFP^+$ cells by intratracheal instillation 3 d before study. Note that most of the GFP staining (*arrows*) seen in the first section (*A*) is also detected in the third section (*C*). The second section (*B*) demonstrates α-SMA immunostaining in many of the same cells (*arrowheads*) as GFP. All panels are the same magnification; short (vertical) dimensions of panels are 436 μm.

cells were not likely the result of cellular fusion. GFP-expression in donor animals decreases with age, suggesting the possibility that GFP-expression may have decreased below levels of detection in some engrafted cells.

Fibroblasts comprise a small percentage of the total cell population recovered by bronchoalveolar lavage in patients with fibrotic lung diseases but are not present in the lavage from normal control subjects (7, 8, 21). During fibrogenic reactions, epithelial cells are damaged and myofibroblasts migrate across gaps in the epithelial basement membrane and between epithelial cells into the alveolar space and proliferate (22). Fibroblasts derived from patients with idiopathic pulmonary fibrosis express α-SMA, whereas fibroblasts derived from patients with sarcoidosis do not (7, 8, 21). These fibroblasts may migrate into the interstitium from the alveolar space; however, the precise mechanisms regulating the transepithelial migration of fibroblasts are unknown. The transepithelial migration of neutrophils into the alveolar space involves the transient opening of epithelial intercellular junctions by a process that is regulated by specific proteins such as occludin (23, 24). It is likely that migration of alveolar fibroblasts follow the same transepithelial process.

Several inflammatory substances, including platelet-derived growth factor, induce chemotaxis for lung fibroblasts *in vitro* (25, 26). In the saline-treated adult wild-type mouse lung, we detected $GFP^+$ cells in interstitial tissues. The $GFP^+$ fibroblasts may gain access to the interstitium in areas with local inflammation where a gradient of chemoattractants exists. Lymphocytes administered endotracheally to normal mice traverse the epithelial cell barrier and appear in regional lymph nodes, suggesting that the mechanisms governing transepithelial migration are bidirectional for lymphocytes and do not require overt lung injury (27). In the elastase-injured lung, engrafted cells were seen in

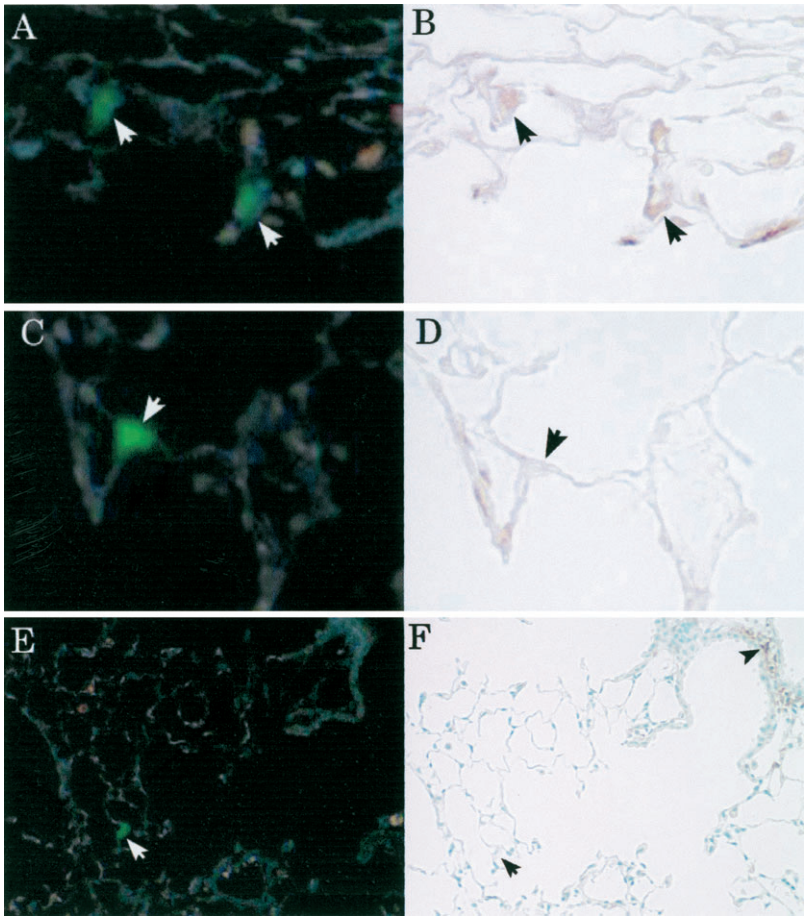


***Figure 8.*** *A, C,* and *E* show GFP$^+$ cells (*white arrows*) in the lungs of wild-type PPE-treated host mice 20 d after an intratracheal instillation of cultured GFP$^+$ cells. *B, D,* and *F* show the same cells (*black arrows*) after immunostaining for α-SMA (α-SMA) (*B* and *D*) and after immunostaining for F4/80 (*F*). *A* and *B* indicate GFP$^+$ cells that are positive for α-SMA, whereas *C* and *D* indicate a GFP$^+$ cell that is not positive for α-SMA. *E* and *F* shows a GFP$^+$ cell that was not positive for F4/80. The *arrowhead* points to F4/80$^+$ stained cells (macrophages) in a parabronchiolar space. *E* and *F* were counterstained with methyl green. *A* and *D* are 80 μm in vertical dimension. *E* and *F* are 290 μm in vertical dimension.

the walls of enlarged airspaces suggesting that remodeling of the airspaces allows increased access to the interstitium.

In the normal adult lung, interstitial fibroblasts are quiescent and do not express detectable levels of elastin or collagen mRNA as assessed by *in situ* hybridization (6). However, fibroblasts appear to function to maintain normal matrix elements. As noted, a recent study demonstrated that LOXL1-deficient mice develop emphysema (3). In culture, neonatal fibroblasts secrete transforming growth factor-β (TGF-β) and respond to exogenous TGF-β with production of connective tissue matrix substances including elastin and collagen (28). We detected GFP$^+$ cells in alveolar walls and interstitial areas. In some areas multiple GFP$^+$ cells were detected, suggesting that these sites were readily available for transepithelial migration or that the cells replicated in these interstitial areas.

Emphysema is characterized by airspace enlargement and loss of cellularity and matrix components in alveolar structures. The mechanisms regulating cellular loss in humans are not known and are likely complex. In rodent models, emphysema is induced by the activation of apoptosis in alveolar walls by inhibition of vascular endothelial growth factor receptors or intratracheal injection of active caspase-3 (29, 30). In the residual tissue of emphysematous lungs, myofibroblast activation results in the deposition of matrix elements; however, this repair is inadequate to restore normal alveolar architecture. An increase in apoptosis occurs in the lungs of individuals with emphysema (31, 32). In our rodent model, engraftment of cells may serve to replace fibroblasts lost from the alveolar wall after elastase injury.

***Conflict of Interest Statement***: None of the authors has a financial relationship with a commercial entity that has an interest in the subject of this manuscript.

## References

1. Snider GL. Emphysema: the first two centuries–and beyond. A historical overview, with suggestions for future research: Part 1. *Am Rev Respir Dis* 1992;146:1334–1344.
2. Snider GL, Lucey EC, Stone PJ. Animal models of emphysema. *Am Rev Respir Dis* 1986;133:149–169.
3. Liu X, Zhao Y, Gao J, Pawlyk B, Starcher B, Spencer JA, Yanagisawa H, Zuo J, Li T. Elastic fiber homeostasis requires lysyl oxidase-like 1 protein. *Nat Genet* 2004;36:178–182.
4. Nakamura T, Lozano PR, Ikeda Y, Iwanaga Y, Hinek A, Minamisawa S, Cheng CF, Kobuke K, Dalton N, Takada Y, *et al.* Fibulin-5/DANCE is essential for elastogenesis *in vivo. Nature* 2002;415:171–175.
5. Karlinsky J, Fredette J, Davidovits G, Catanese A, Snider R, Faris B, Snider GL, Franzblau C. The balance of lung connective tissue elements in elastase-induced emphysema. *J Lab Clin Med* 1983;102:151–162.
6. Lucey EC, Goldstein RH, Stone PJ, Snider GL. Remodeling of alveolar walls after elastase treatment of hamsters: results of elastin and collagen mRNA *in situ* hybridization. *Am J Respir Crit Care Med* 1998;58: 555–564.
7. Fireman E, Kivity S, Shahar I, Reshef T, Mekori YA. Secretion of stem cell factor by alveolar fibroblasts in interstitial lung diseases. *Immunol Lett* 1999;67:229–236.
8. Shahar I, Fireman E, Topilsky M, Grief J, Schwarz Y, Kivity S, Ben-Efraim S, Spirer Z. Effect of endothelin-1 on alpha-smooth muscle actin expression and on alveolar fibroblasts proliferation in interstitial lung diseases. *Int J Immunopharm.* 1999;21:759–775.
9. Berk JL, Franzblau C, Goldstein RH. Recombinant interleukin-1 beta inhibits elastin formation by a neonatal rat lung fibroblast subtype. *J Biol Chem* 1991;266:3192–3197.
10. Kuang PP, Goldstein RH. Regulation of elastin gene transcription by

interleukin-1 beta-induced C/EBP beta isoforms. *Am J Physiol Cell Physiol* 2003;285:C1349–C1355.
11. Amy RW, Bowes D, Burri PH, Haines J, Thurlbeck WM. Postnatal growth of the mouse lung. *J Anat* 1977;124:131–151.
12. Burri PH, Dbaly J, Weibel ER. The postnatal growth of the rat lung: I. Morphometry. *Anat Rec* 1974;178:711–730.
13. Lucey E, Keane J, Kuang P-P, Snider GL, Goldstein RH. Severity of elastase induced emphysema is decreased in TNF-α and IL-1β receptor deficient mice. *Lab Invest* 2002;82:79–85.
14. Schilling M, Besselmann M, Leonhard C, Mueller M, Ringelstein EB, Kiefer R. Microglial activation precedes and predominates over macrophage infiltration in transient focal cerebral ischemia: a study in green fluorescent protein transgenic bone marrow chimeric mice. *Exp Neurol* 2003;183:25–33.
15. Roy SG, Nozaki Y, Phan SH. Regulation of alpha-smooth muscle actin gene expression in myofibroblast differentiation from rat lung fibroblasts. *Int J Biochem Cell Biol.* 2001;33:723–734.
16. Kotton DN, Ma BY, Cardoso WV, Sanderson EA, Summer RS, Williams MC, Fine A. Bone marrow-derived cells as progenitors of lung alveolar epithelium. *Development* 2001;128:5181–5188.
17. Hashimoto N, Jin H, Liu T, Chensue SW, Phan SH. Bone marrow-derived progenitor cells in pulmonary fibrosis. *J Clin Invest* 2004;113:243–252.
18. Suda A, Takiguchi Y, Omori S, Miyazawa H, Sugimoto T, Kurosu K, Tatsumi K, Tanabe N, Kuriyama T. Gene delivery to the lung by means of syngeneic fibroblasts: an experimental model. *Exp Lung Res* 2003;29:227–241.
19. Nygren JM, Jovinge S, Breitbach M, Sawen P, Roll W, Hescheler J, Taneera J, Fleischmann BK, Jacobsen SE. Bone marrow-derived hematopoietic cells generate cardiomyocytes at a low frequency through cell fusion, but not transdifferentiation. *Nat Med* 2004;10:494–501.
20. Terada N, Hamazaki T, Oka M, Hoki M, Mastalerz DM, Nakano Y, Meyer EM, Morel L, Petersen BE, Scott EW. Bone marrow cells adopt the phenotype of other cells by spontaneous cell fusion. *Nature* 2002;416:542–545.
21. Fireman E, Shahar I, Shoval S, Messer G, Dvash S, Grief J. Morphological and biochemical properties of alveolar fibroblasts in interstitial lung diseases. *Lung* 2001;179:105–117.
22. Crouch E. Pathobiology of pulmonary fibrosis. *Am J Physiol* 1990;259: L159–L184.
23. Burns AR, Smith CW, Walker DC. Unique structural features that influence neutrophil emigration into the lung. *Physiol Rev* 2003;83:309–336.
24. Huber D, Balda MS, Matter K. Occludin modulates transepithelial migration of neutrophils. *J Biol Chem* 2000;275:5773–5778.
25. Osornio-Vargas AR, Lindroos PM, Coin PG, Badgett A, Hernandez-Rodriguez NA, Bonner JC. Maximal PDGF-induced lung fibroblast chemotaxis requires PDGF receptor-alpha. *Am J Physiol* 1996;271: L93–L99.
26. Shure D, Senior RM, Griffin GL, Deuel TF. PDGF AA homodimers are potent chemoattractants for fibroblasts and neutrophils, and for monocytes activated by lymphocytes or cytokines. *Biochem Biophys Res Commun* 1992;186:1510–1514.
27. Lehmann C, Wilkening A, Leiber D, Markus A, Krug N, Pabst R, Tschernig T. Lymphocytes in the bronchoalveolar space reenter the lung tissue by means of the alveolar epithelium, migrate to regional lymph nodes, and subsequently rejoin the systemic immune system. *Anat Rec* 2001; 264:229–236.
28. McGowan SE, Jackson SK, Olson PJ, Parekh T, Gold LI. Exogenous and endogenous transforming growth factors-beta influence elastin gene expression in cultured lung fibroblasts. *Am J Respir Cell Mol Biol* 1997;17:25–35.
29. Kasunori K, Rubin MT, Taraseviciene-Steward L, Le Cras TD, Abman S, Hirth PK, Waltenberger J, Voelkel NF. Inhibition of VEGF receptors causes lung cell apoptosis and emphysema. *J Clin Invest* 2000;106: 1311–1319.
30. Aoshiba K, Yokohori N, Nagai A. Alveolar wall apoptosis causes lung destruction and emphysematous changes. *Am J Respir Cell Mol Biol* 2003;28:555–562.
31. Yokohori N, Aoshiba K, Nagai A. Increased levels of cell death and proliferation in alveolar wall cells in patients with pulmonary emphysema. *Chest* 2004;125:626–632.
32. Segura-Valdez L, Pardo A, Gaxiola M, Uhal BD, Becerril C, Selman M. Up-regulation of gelatinases A and B, collagenases 1 and 2, and increased parenchymal cell death in COPD. *Chest* 2000;117:684–694.